Low Fractal Dimension Cluster-Dilute Soot Aggregates from a Premixed Flame

Rajan K. Chakrabarty,[1,2,*] Hans Moosmüller,[1] W. Patrick Arnott,[3,1] Mark A. Garro,[1,4] Guoxun Tian,[1,3] Jay G. Slowik,[5] Eben S. Cross,[6] Jeong-Ho Han,[6] Paul Davidovits,[6] Timothy B. Onasch,[7] and Douglas R. Worsnop[7]

[1]*Desert Research Institute, Nevada System of Higher Education, Reno, Nevada 89512, USA*
[2]*Chemical Physics Program, University of Nevada, Reno, Nevada 89557, USA*
[3]*Department of Physics, University of Nevada, Reno, Nevada 89557, USA*
[4]*Division of Engineering and Applied Sciences, Harvard University, Cambridge, Massachusetts 02138, USA*
[5]*Department of Chemistry, University of Toronto, Toronto, Ontario M5S 3H6, Canada*
[6]*Department of Chemistry, Boston College, Chestnut Hill, Massachusetts 02467, USA*
[7]*Aerodyne Research Inc., Billerica, Massachusetts 01821, USA*

(Received 20 November 2008; published 12 June 2009)

Using a novel morphology segregation technique, we observed minority populations (≈3%) of submicron-sized, cluster-dilute fractal-like aggregates, formed in the soot-formation window (fuel-to-air equivalence ratio of 2.0–3.5) of a premixed flame, to have mass fractal dimensions between 1.2 and 1.51. Our observations disagree with previous observations of a universal mass fractal dimension of ≈1.8 for fractal-like aerosol aggregates formed in the dilute-limit via three-dimensional diffusion-limited cluster aggregation processes. A hypothesis is presented to explain this observation. Subject to verification of this hypothesis, it may be possible to control the fractal dimension and associated properties of aggregates in the cluster-dilute limit through application of a static electric field during the aggregation process.

DOI: 10.1103/PhysRevLett.102.235504 PACS numbers: 61.43.Hv, 64.60.al, 81.20.Rg, 82.70.Rr

Combustion-generated carbonaceous aerosols including fractal-like soot particles influence Earth's radiation balance and climate [1], atmospheric chemistry [2], visibility [3], and the health of living beings including humans [4] on scales ranging from local to global. Fractal-like aggregates (FAs) also play an important role in the aggregation of interstellar dust [5] and in the large-scale industrial production of nanomaterials with flame synthesis [6].

It is now well established that the formation of cluster-dilute aerosols and colloids in flames proceeds via a three-dimensional (3D) diffusion-limited cluster aggregation (DLCA) growth mechanism, which is governed by the Smoluchowski equation [7–9]. Cluster dilute refers to the average cluster-cluster separation being much larger than the cluster size [7]. Aggregation of monomers (repeating units) via diffusion forms FAs whose mass to linear size (radius of gyration) relationship can be written as a power law

$$N = k_0 (R_g/d_p)^{D_f}, \quad (1)$$

where N is the number of monomers, D_f is the mass fractal dimension, R_g is the aggregate radius of gyration, k_0 is the fractal prefactor, and d_p is the mean monomer diameter. D_f describes the space-filling characteristics of the aggregate [10]. Starting with Forrest and Witten [11], numerous experimental and simulation studies have used Eq. (1) to characterize the structure of FAs from various sources in the cluster-dilute limit. Without exception, all studies have reported D_f in the range of 1.7–1.8 [7,12,13].

In this Letter, we report the first observation of ensembles of cluster-dilute soot FAs with much lower D_f (i.e., 1.2–1.5). The soot FAs were produced in the soot-formation window [14] of a premixed ethene (C_2H_4)-oxygen (O_2) flame. An established charge-based particle segregation technique [15,16] was used to segregate elongated FAs for morphology analysis with scanning electron microscopy (SEM) and image processing techniques.

The ethene-oxygen premixed flame setup (Fig. 1) used for producing soot FAs has previously been described in detail [17,18]. The mass flow rates of ethene and oxygen were varied to operate the flame with four fuel-rich fuel-to-air equivalence ratios φ—2.3, 2.8, 3.5, and 5.0 [19]. For each φ, soot FAs were sampled in the overfire region of the flame, where the characteristic flame residence times are

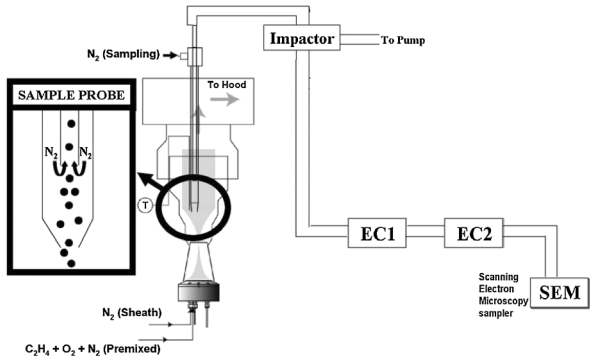

FIG. 1. Schematic diagram of the experimental setup used for soot aggregate generation and characterization.

roughly an order of magnitude longer than the laminar smoke point residence time. Soot particle monomer number concentration in the long residence time regime is independent of axial position, which facilitates sampling of a steady and uniform distribution of particles. Sampled soot particles were passed through an impactor to remove particles larger than ≈ 5 μm in diameter. Particle flow exiting the impactor was directed through two identical electrostatic classifiers (ECs) in series (Fig. 1). The EC utilizes a combination of a viscous and electrostatic force to select a combination of net charge q and electrical mobility diameter D_m with a spatial gate. ECs are widely used for particle sizing and for the generation of monodisperse aerosols in the size range from 0.005 to 1.0 μm [20]. The particles were bipolarly charged using a neutralizer (model Kr-85, TSI Inc., St. Paul, MN) before entering either of the ECs (model 3080, TSI Inc., St. Paul, MN).

A detailed description of the morphology segregation technique has been given previously [15] and only some relevant points are discussed below. This technique is based on the fact that more elongated particles are more likely to become doubly charged than more compact particles of the same mass because it requires less energy to add the second charge at a larger distance from the first one. The sheath flow rate of the first EC was set at around 8 ($1\,\mathrm{min}^{-1}$) STP to select singly charged (i.e., $q = -e$) particles with electrical mobility diameter $D_m \approx 280$ nm and doubly charged (i.e., $q = -2e$) particles with $D_m = 460$ nm. The particles exiting the first EC were neutralized and sent to the second EC, which was set to select singly charged particles with $D_m = 460$ nm. The particles selected by the second EC are the same 460 nm particles that were originally selected by the first EC with a net double charge on them. This technique of shape selecting particles only works if the sample contains enough particles, with a morphology facilitating the placement of double charges, in the desired size range. In samples containing particles with near-alike morphologies, this charge-based morphology separation technique fails. For example, unsuccessful attempts were made to segregate morphologies of FAs with $D_m < 200$ nm from our premixed flame. The majority of these doubly charged, small FAs ($D_m < 200$ nm) had $D_f \approx 1.8$, typical of 3D FAs. These small FAs consist of only few monomers resulting in a more limited number of possible shapes. Unlike FAs with a large number of monomers, small FAs have a more spherical morphology with little opportunity for segregating more spherical from more elongated aggregates. Therefore, the particle number concentration exiting the second EC was a very small fraction of the sample population [15].

In this study, the combination of two ECs segregated more elongated FAs, constituting $\approx 3\%$ of the total submicron-sized particles sampled from the flame [21]. The segregated particle size distribution from the EC is Gaussian with a peak of $D_m \approx 460$ nm [15]. Soot particles exiting the second EC were impacted with a flow rate of 2 ($1\,\mathrm{min}^{-1}$) STP onto 10-μm thick nuclepore clear polycarbonate filters for SEM analysis. It has been observed during past studies [17,22] that the original particle structure of impaction-collected FAs is modified only very minimally upon impaction onto the filter at the pump-suction flow rate used in this study. After sampling, the filter samples were kept in refrigerated storage and later prepared for SEM analysis by coating them with a 1-nm thick layer of platinum to prevent aerosol charging during SEM analysis. The coated filters were analyzed using a Hitachi scanning electron microscope (model S-4700) [17,22].

For each φ, images of ≈ 150 individual doubly charged particles were analyzed for their D_f. For a 3D FA in the cluster-dilute regime, parts of the aggregate can randomly screen other parts during two-dimensional (2D) imaging [13,23]. After correcting for this screening, the projected 2D D_f of FAs approximately equals their actual 3D D_f for 3D fractal dimensions smaller than 2 [8,24]. The 3D monomer number N in Eq. (1) can be calculated from the 2D projected image using the equation [23,25]

$$N = \left(\frac{A_{\mathrm{agg}}}{A_{\mathrm{mon}}}\right)^{\kappa}, \tag{2}$$

where $\kappa = 1.10$ corrects for the 2D screening effect, A_{agg} is the 2D aggregate projected area, and A_{mon} is the mean projected monomer area. It is noteworthy to mention here that accurate estimation of N from the SEM images is almost impossible for this study, especially since the aggregates were coated with a significant amount of organic carbon produced from the flame. The FA properties quantified using image analysis include A_{agg}, A_{mon}, L (projected aggregate length), and W (aggregate projected width normal to L) [17,22]. Monomers clearly distinguishable in aggregates were selected and their diameters were measured. The number size distributions of monomers from each set of experiments could be described by monomodal log-normal size distributions with mean monomer diameters ranging between 37 and 43 nm, and a standard deviation of ≈ 5 nm. The parameter $(LW)^{0.5}$—defined as the geometric mean diameter of an aggregate—has been shown [26] to be a good approximate for R_g, and Eq. (1) can be rewritten as

$$N \sim [\sqrt{LW}]^{D_f}. \tag{3}$$

Figure 2 shows N vs $(LW)^{0.5}$ data plotted on a log-log scale for the doubly charged soot FAs with an electrical mobility diameter $D_m = 460$ nm and for three φ's (i.e., 2.3, 2.8, and 3.5). On the log-log scale, there is a clear linear relationship between N and $(LW)^{0.5}$. The slope of this relationship is the mass fractal dimension D_f, which is determined with a linear least-squares fit. As φ is increased from 2.3 to 3.5, D_f monotonically decreases from 1.51 to 1.20. Upon further increase of φ to 5.0, the particles become near-spherical with $D_f \approx 3$ [Fig. 3(d)] due to

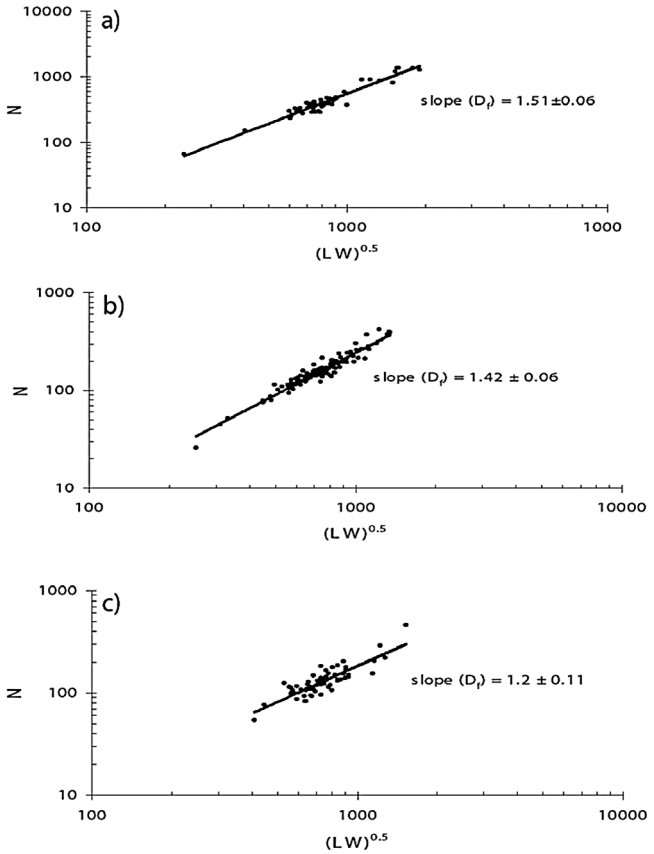

FIG. 2. Mass fractal dimension D_f of morphology segregated, $D_m = 460$ nm soot aggregates generated with fuel-to-air equivalence ratios φ of (a) $\varphi = 2.3$, (b) $\varphi = 2.8$, and (c) $\varphi = 3.5$.

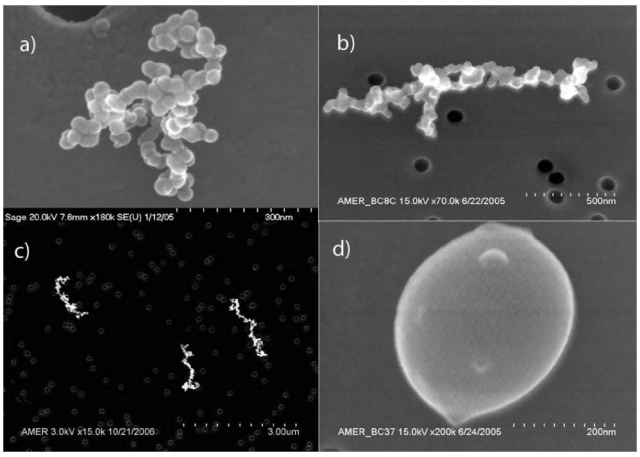

FIG. 3. (a) A commonly observed soot particle with $D_f \approx 1.8$ formed by 3D DLCA (not from this study), (b) a typical soot particle observed with $D_f = 1.2$ ($\varphi = 3.5$) in this study, and (c) soot particles with $D_f = 1.51$ ($\varphi = 2.3$). These aggregates look elongated and "stringy" in comparison to the more common aggregate in (a). (d) At high $\varphi \approx 5.0$ soot particles in our premixed flame lose their fractal nature and become near-spherical particles.

condensation of organics emitted by the flame. These results contain two novel features: (i) low D_f much smaller than the typical 1.8 are, for the first time, observed in a premixed flame, and (ii) D_f is a function of φ, monotonically decreasing with increasing φ in the range of 2.3–3.5.

Most simulation studies have investigated aggregation of neutrally charged particle populations due to Brownian motion, and have found that the fractal dimension of the resulting aggregates had a narrow distribution centered around 1.8 in the asymptotic, equilibrium limit. These findings lead us to conclude that the observed low fractal dimensions in this study are not statistical outliers of a broad distribution of fractal dimensions. The observation of D_f much smaller than the 1.8 typical for 3D DLCA can possibly be explained by the following mechanism: the electric field inside a flame causes partial alignment of aggregates with a dipole moment and non-Brownian diffusion of charged monomers during the aggregation process.

The possibility of an electric field in the flame orienting aggregates and aligning the movement of monomers during the aggregation process, thereby reducing its dimensionality, has previously been shown to have led to the formation of aluminum FAs with low D_f of ≈1.6 in flame synthesis [27]. In addition, simulation of the dipole-charge aggregation in a dust plasma has been shown to yield low fractal dimensions with large standard deviations [5]. Studies on aggregation of artificially coated magnetic particles under the influence of long-range dipole moments have also reported low D_f of ≈1.16 [28,29]. While aggregation of particles has been studied extensively with numerical simulations [30,31], very few studies have examined the effects of combustion particle charges, dipole moments, and electrical fields on aggregation. Four decades ago, the seminal research by Weinberg and colleagues was one of the first to investigate the influence of electrical fields on aerosol formation and control [32]. The ionic or charged environment of a flame can give rise to a distribution of monomer and aggregate charge due to the random nature of the charging process [27]. Such a charge distribution increases the rate of aggregation above that of neutral particles and aggregates [33]. Large FAs, in flames, often have a dipole moment that tends to align these aggregates parallel to electric field lines, which is parallel to the preferential direction of movement for charged monomers [27,34]. If electric forces were dominant and all aggregates had dipole moments and all monomers were charged, one would expect near-linear shaped FAs (i.e., linear chains with $D_f \approx 1$) to be formed. However, in a flame environment not all particles are necessarily charged or have dipole moments and the effect of alignment of particles and their movement competes with Brownian motion. This may result in a majority population of aggregates formed through 3D DLCA with a D_f of ≈1.8 [Fig. 3(a)] and a minority population with a lower D_f as observed here. Based on the competition of random

Brownian motion with alignment due to electrostatic forces one would expect to see more chainlike aggregates with a lower fractal dimension at lower aggregation temperatures. This is exactly what is observed here. Increasing φ of our premixed flame lowers the flame temperature [19] and thereby lowers the D_f as observed (Fig. 2).

We also observed that at extremely fuel-rich conditions (i.e., $\varphi \approx 5$), particles produced by the flame had near-spherical shapes [i.e., $D_f \approx 3$; see Fig. 3(d)]. Slowik *et al.* [35] observed a similar phenomenon, and noted that as φ increases to above 4.0 in their premixed flame, a sharp transition in particle properties occurs including a drastic increase of the ratio of polycyclic aromatic hydrocarbons (PAHs) to black carbon and an increase of the mass fractal dimension from 1.7 ± 0.15 to 2.95 ± 0.10. Their explanation for this observation was that as the concentration of PAHs in a flame increases beyond a certain limit, the pores and irregularities of the FA get filled by the condensed PAH compounds and the individual monomers lose their identity. At this transition point the FAs become nearly smooth spheres.

In summary, we segregated a small population ($\approx 3\%$) of submicron-sized (≈ 460 nm) soot FAs produced in the soot-formation window of a premixed ethene-oxygen flame, and observed their D_f to be unusually low (i.e., between 1.2 and 1.5). We hypothesize that their formation mechanism may have been influenced by electrostatic forces inside of a flame, thereby explaining their extremely low D_f. The electrostatic force hypothesis could also explain the observed decrease of D_f with the increasing φ of the flame.

Further investigation of the mechanisms involved in the production of low fractal dimension aggregates is clearly needed for understanding the properties of combustion aerosols, industrially produced black carbon, and interstellar dust aggregates. If the electrostatic force hypothesis can be verified, it may be possible to control the fractal dimension and associated properties of soot through application of a static electric field.

This work has been supported in part by U.S. DOE ASP Grant No. DE-FG02-05ER64008. R. K. C. and M. A. G. acknowledge the support received from the National Science Foundation (Grant No. 0447416) for carrying out this research work.

*Corresponding author.
Rajan.Chakrabarty@dri.edu

[1] J. M. Haywood and V. Ramaswamy, J. Geophys. Res. **103**, 6043 (1998).
[2] B. J. Finlayson-Pitts and J. N. Pitts, *Chemistry of the Upper and Lower Atmosphere: Theory, Experiments, and Applications* (Academic, San Diego, 2000).
[3] J. G. Watson, J. Air Waste Manage. Assoc. **52**, 626 (2002).
[4] S. Vedal, J. Air Waste Manage. Assoc. **47**, 551 (1997).
[5] L. S. Matthews and T. W. Hyde, IEEE Trans. Plasma Sci. **32**, 586 (2004).
[6] S. K. Friedlander, *Smoke, Dust, and Haze* (Wiley-Interscience, New York, 1977).
[7] R. Dhaubhadel *et al.*, Phys. Rev. E **73**, 011404 (2006).
[8] R. Jullien and R. Botet, *Aggregation and Fractal Aggregates* (World Scientific, Singapore, 1987).
[9] R. Jullien, M. Kolb, and R. Botet, J. Phys. (Paris) **45**, 395 (1984).
[10] K. A. Katrinak *et al.*, Environ. Sci. Technol. **27**, 539 (1993).
[11] S. R. Forrest and T. A. Witten, J. Phys. A **12**, L109 (1979).
[12] C. M. Sorensen, Aerosol Sci. Technol. **35**, 648 (2001).
[13] C. M. Sorensen and W. B. Hageman, Langmuir **17**, 5431 (2001).
[14] M. J. Height *et al.*, Carbon **42**, 2295 (2004).
[15] R. K. Chakrabarty *et al.*, J. Aerosol Sci. **39**, 785 (2008).
[16] A. Zelenyuk and D. Imre, Aerosol Sci. Technol. **41**, 112 (2007).
[17] R. K. Chakrabarty *et al.*, Appl. Opt. **46**, 6990 (2007).
[18] J. G. Slowik *et al.*, Aerosol Sci. Technol. **41**, 295 (2007).
[19] S. R. Turns, *An Introduction to Combustion: Concepts and Applications* (McGraw-Hill, New York, 1996).
[20] E. O. Knutson and K. T. Whitby, J. Aerosol Sci. **6**, 443 (1975).
[21] *Manual for the Series 3080 Electrostatic Classifiers* (TSI, Minnesota, 2006).
[22] R. K. Chakrabarty *et al.*, J. Geophys. Res. **111**, D07204 (2006).
[23] C. Oh and C. M. Sorensen, J. Colloid Interface Sci. **193**, 17 (1997).
[24] R. Jullien, R. Thouy, and F. Ehrburger-Dolle, Phys. Rev. E **50**, 3878 (1994).
[25] Ü. Ö. Köylü *et al.*, Combust. Flame **100**, 621 (1995).
[26] R. J. Samson, G. W. Mulholland, and J. W. Gentry, Langmuir **3**, 272 (1987).
[27] V. V. Karasev *et al.*, Combust. Explos. Shock Waves **37**, 734 (2001).
[28] G. Helgesen *et al.*, Phys. Rev. Lett. **61**, 1736 (1988).
[29] P. M. Mors, R. Botet, and R. Jullien, J. Phys. A **20**, L975 (1987).
[30] M. Kostoglou and A. G. Konstandopoulos, J. Aerosol Sci. **32**, 1399 (2001).
[31] R. D. Mountain and G. W. Mulholland, Langmuir **4**, 1321 (1988).
[32] F. J. Weinberg, Proc. R. Soc. A **307**, 195 (1968).
[33] T. Matsoukas, J. Colloid Interface Sci. **187**, 474 (1997).
[34] B. M. Smirnov, *Physics of Fractal Clusters* (Nauka, Moscow, 1991), in Russian.
[35] J. G. Slowik *et al.*, Aerosol Sci. Technol. **38**, 1206 (2004).